

## Diacetoneglucose Complexes of Manganese(II) and Iron(II) and Their Organometallic Derivatization

Umberto Piarulli<sup>†</sup> and Carlo Floriani\*

Institut de Chimie Minérale et Analytique, BCH, Université de Lausanne, CH-1015 Lausanne, Switzerland

Nazzareno Re

Dipartimento di Chimica, Università di Perugia, I-06100 Perugia, Italy

Giuliana Gervasio and Davide Viterbo

Dipartimento di Chimica I.F.M., Università di Torino, I-10125 Torino, Italy

Received March 17, 1998

Homoleptic metal–sugar complexes were obtained in the form of Mn<sup>II</sup>– and Fe<sup>II</sup>–diacetoneglucose derivatives. The protolysis of [Mn<sub>3</sub>Mes<sub>6</sub>] and [Fe<sub>2</sub>Mes<sub>4</sub>] (Mes = 2,4,6-Me<sub>3</sub>C<sub>6</sub>H<sub>2</sub>) with DAGH (1,2:5,6-di-*O*-isopropylidene- $\alpha$ -D-glucopyranose, diacetoneglucose) led to [M(DAG)<sub>2</sub>] [M = Mn (**1**), Fe (**2**)]. Although monomeric in solution, they showed a different degree of aggregation in the solid state, iron being monomeric and manganese oligomeric (see magnetic properties). Dimeric complexes from **1** and **2** were obtained in the reaction with 9,10-phenanthroline [phen], leading to [(phen)<sub>2</sub>M( $\mu$ -DAG)<sub>2</sub>M(DAG)<sub>2</sub>] [M = Mn (**3**), Fe (**4**)]. The organometallic functionalization of **1** and **2** was achieved *via* a ligand redistribution reaction mixing them with [Mn<sub>3</sub>Mes<sub>6</sub>] and [Fe<sub>2</sub>Mes<sub>4</sub>], respectively. The reaction led to mixed alkoxo aryl trinuclear complexes in the form of [(Mes)<sub>2</sub>M<sub>2</sub>( $\mu$ -DAG)<sub>2</sub>M( $\mu$ -Mes)<sub>2</sub>] [M = Mn (**5**), Fe (**6**)]. Both have a linear trimetallic skeleton with Mn $\cdots$ Mn and Fe $\cdots$ Fe average distances of 2.93 and 2.88 Å, respectively. The crystal data are as follows: complex **5**, C<sub>60</sub>H<sub>82</sub>Mn<sub>3</sub>O<sub>12</sub>, monoclinic, space group *P*2<sub>1</sub>, *a* = 10.289(5) Å, *b* = 20.878(5) Å, *c* = 14.015(5) Å,  $\beta$  = 93.19(2)°, *Z* = 2; complex **6**, C<sub>60</sub>H<sub>82</sub>Fe<sub>3</sub>O<sub>12</sub>, monoclinic, space group *P*2<sub>1</sub>, *a* = 9.748(12) Å, *b* = 26.05(3) Å, *c* = 12.50(2) Å,  $\beta$  = 107.50(2)°, *Z* = 2. The data were collected at –123 °C. For **5** and **6** the magnetic analysis showed a strong antiferromagnetic coupling between the M(II) centers, with spin frustration leading to an overall *S* = 5/2 and *S* = 2 ground state, respectively.

### Introduction

Although carbohydrates in their monomeric form have a quite large number of attractive structural, stereochemical, and chemical peculiarities, their use in combination with metals for entering novel molecular architectures, or as unique ancillary ligands in organometallic chemistry is very limited.<sup>1</sup> As far as the first of these uses is concerned, homoleptic complexes containing the deprotonated form of diacetoneglucose (DAG) have been recently studied, in their neutral<sup>2</sup> [M(DAG)<sub>*n*</sub>] or anionic form [M(DAG)<sub>*m*</sub>]<sup>*q*-</sup>. In the latter case, the anionic forms

function as metallohosts for alkali metal cations.<sup>3</sup> Concerning the use of carbohydrates in organometallic chemistry, we should mention a quite successful precedent, namely [CpTi(DAG)<sub>2</sub>Cl] [Cp =  $\eta^5$ -C<sub>5</sub>H<sub>5</sub>] which assisted the enantioselective formation of C–C bonds in aldol condensations and allylation of aldehydes.<sup>4</sup> In the so far reported Ti<sup>–4</sup> and Mg–DAG<sup>5</sup> derivatives, however, the metal functions essentially as a chiral Lewis acid. A domain thus far largely unexplored is the use of sugars, and particularly DAGH, for managing the chemistry of the M–C functionalities. This is particularly surprising in the case of early transition metals having such a rich organometallic chemistry based on alkoxo and aryloxo ligands.<sup>6</sup> In fact, DAGH (1,2:

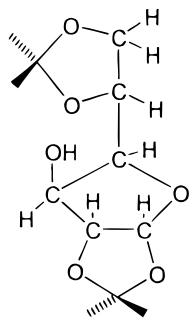
\* To whom correspondence should be addressed.

<sup>†</sup> Present address: Dipartimento di Chimica Organica e Industriale, Università di Milano, Via Venezian 21, I-20133 Milano, Italy.

- (1) (a) Piarulli, U.; Floriani, C. In *Progress in Inorganic Chemistry*; Karlin, K., Ed.; Wiley: New York, 1997; Vol. 45, p 393 and references therein. (b) Verchè, J.-F.; Chappelle, S.; Xin, F.; Crans, D. C. In *Progress in Inorganic Chemistry*; Karlin, K., Ed.; Wiley: New York, 1988; Vol. 47, p 837.
- (2) (a) Ruiz, J.; Floriani, C.; Chiesi-Villa, C.; Guastini, C. *J. Chem. Soc., Dalton Trans.* **1991**, 2467. (b) Williams, D. N.; Piarulli, U.; Floriani, C.; Chiesi-Villa, A.; Rizzoli, C. *J. Chem. Soc., Dalton Trans.* **1994**, 1243. (c) Piarulli, U.; Williams, D. N.; Floriani, C.; Gervasio, D.; Viterbo, D. *J. Organomet. Chem.* **1995**, 503, 185. (d) Piarulli, U.; Williams, D. N.; Floriani, C.; Gervasio, D.; Viterbo, D. *J. Chem. Soc., Dalton Trans.* **1995**, 3329.

- (3) (a) Piarulli, U.; Williams, D. N.; Floriani, C.; Gervasio, D.; Viterbo, D. *J. Chem. Soc., Chem. Commun.* **1994**, 1409. (b) Piarulli, U.; Rogers, A. J.; Floriani, C.; Gervasio, D.; Viterbo, D. *Inorg. Chem.* **1997**, 36, 6127.
- (4) (a) Duthaler, R. O.; Hafner, A. *Chem. Rev.* **1992**, 92, 807. (b) Duthaler, R. O.; Herold, P.; Lottenbach, W.; Oertle, K.; Riediker, M. *Angew. Chem., Int. Ed. Engl.* **1989**, 28, 495. (c) Bold, G.; Riediker, M.; Duthaler, R. O. *Angew. Chem., Int. Ed. Engl.* **1989**, 28, 497. (d) Riediker, M.; Duthaler, R. O. *Angew. Chem., Int. Ed. Engl.* **1989**, 28, 494. (e) *Organic Synthesis via Organometallics*; Dötz, K. H., Hoffmann, R. W., Eds.; Vieweg: Braunschweig, Germany, 1991.
- (5) Inch, T. D.; Lewis, G. J.; Sainsbury, G. L.; Sellers, D. J. *Tetrahedron Lett.* **1969**, 41, 3657.

Chart 1



5,6-di-*O*-isopropylidene- $\alpha$ -D-glucopyranose, or diacetoneglucose) (Chart 1) should in principle be considered as a mono-functional alcohol. In addition, the alkoxy chemistry of early transition metals makes available the synthetic methodology for accessing the M–C chemistry using [(DAG) $_n$ MX $_m$ ] functionalizable complexes, with the great advantage, in the latter case, of having chiral ligands around the metal.<sup>4</sup> The chemistry and, particularly, the organometallic chemistry of middle and late transition metals based on alkoxy ancillary ligands is much more difficult to approach due to the lack of a reasonable number of precedents in the literature.<sup>7</sup> We report here the synthesis of homoleptic manganese(II) and iron(II) diacetoneglucose derivatives and a synthetic methodology, based on the ligand redistribution reaction, for achieving their organometallic functionalization.

## Experimental Section

**General Procedure.** All reactions were carried out under a purified nitrogen atmosphere using Schlenk and vacuum line techniques. A Braun Dry Box was used for the preparation of Nujol mulls for oxygen-sensitive samples and for mounting crystals. Solvents were dried by standard methods then distilled under nitrogen. Infrared spectra were recorded on a Perkin-Elmer 1600 FT infrared spectrophotometer (Nujol mulls between 4000 and 400 cm<sup>-1</sup> using KBr plates). Microanalyses were performed on a Carlo Erba EA 1108 CHNS-O at the University of Lausanne. Magnetic susceptibility measurements were made on a MPMS5 SQUID susceptometer (Quantum Design Inc.) operating at a magnetic field strength of 3 kG. Corrections were applied for diamagnetism calculated from Pascal constants. Effective magnetic moments were calculated by the equation  $\mu_{\text{eff}} = 2.828(\chi_M T)^{1/2}$  where

$\chi_M$  is the magnetic susceptibility per metal ion. The fitting of magnetic data to the theoretical expression was performed by minimizing the agreement factor, defined as

$$R = \sum \frac{[\chi_i^{\text{obsd}} - \chi_i^{\text{calcd}}]^2}{(\chi_i^{\text{obsd}})^2}$$

through a Levenberg–Marquardt routine.<sup>8</sup>

**Synthesis of 1.** Using a pressure-equalized dropping funnel, a DAGH (11.1 g, 42.65 mmol) solution in toluene (200 mL) was added dropwise to a suspension of Mn<sub>3</sub>Mes<sub>6</sub>·C<sub>7</sub>H<sub>8</sub><sup>9</sup> (6.90 g, 7.11 mmol) in toluene (100 mL). An immediate reaction ensued, and a pale yellow solution was stirred overnight. Evaporation of toluene under reduced pressure and with the addition of 100 mL of *n*-hexane afforded a cloudy solution which was filtered and stored at –25 °C for 24 h. A white precipitate was then collected on a cold filter and dried under vacuum (9.67 g, 79%). Anal. Calcd for **1**, C<sub>24</sub>H<sub>38</sub>MnO<sub>12</sub>: C, 50.26; H, 6.63. Found: C, 50.13; H, 7.06. MW (cryoscopy in benzene): calcd 573, found 687.

**Synthesis of 2.** A solution of DAGH (9.33 g, 35.86 mmol) in toluene (150 mL), was added dropwise to a cold (–50 °C) solution of [Fe<sub>2</sub>Mes<sub>4</sub>]<sup>10</sup> (5.29 g, 8.95 mmol) in toluene (100 mL). An immediate reaction ensued to yield a greenish solution which was warmed back to room temperature and stirred overnight. Toluene was then evaporated under reduced pressure and *n*-hexane (150 mL) was added. The resulting cloudy solution was filtered, and the filtrate was stored at –25 °C for 24 h. A green precipitate resulted which was collected on a cold filter and dried under vacuum (8.82 g, 86%). Anal. Calcd for **2**, C<sub>24</sub>H<sub>38</sub>FeO<sub>12</sub>: C, 50.18; H, 6.62. Found: C, 50.42; H, 6.96. MW (cryoscopy in benzene): calcd 574, found 584.

**Synthesis of 3.** Using a pressure-equalized dropping funnel, a solution of 1,10-phenanthroline (0.85 g, 4.69 mmol) in toluene (150 mL) was added dropwise to a solution of **1** (2.62 g, 4.57 mmol) in toluene (100 mL). Immediately a deep orange solution formed which, after standing overnight yielded colorless crystals of **3** (2.39 g, 60%). Anal. Calcd for **3**, C<sub>72</sub>H<sub>92</sub>Mn<sub>2</sub>N<sub>4</sub>O<sub>24</sub>: C, 61.27; H, 6.52; N, 3.97. Found: C, 61.39; H, 6.76; N, 3.81.

**Synthesis of 4.** Using a pressure-equalized dropping funnel, a solution of 1,10-phenanthroline (0.56 g, 3.08 mmol) in toluene (50 mL) was added dropwise to a solution of **2** (1.77 g, 3.08 mmol) in toluene (50 mL). The solution turned purple and then deep blue during the addition, and by the end a blue oily solid separated. The reaction mixture was stirred overnight at room temperature, and a deep blue solid in an almost colorless solution resulted. The solid was collected on a filter and dried (1.95 g, 79%). Anal. Calcd for **4**·C<sub>7</sub>H<sub>8</sub>, C<sub>79</sub>H<sub>100</sub>Fe<sub>2</sub>N<sub>4</sub>O<sub>24</sub>: C, 59.59; H, 6.28; N, 3.52. Found: C, 59.42; H, 6.29; N, 3.38.

**Synthesis of 5.** Mn<sub>3</sub>Mes<sub>6</sub>·C<sub>7</sub>H<sub>8</sub> (2.31 g, 2.38 mmol) was added portionwise to a solution of **1** (2.04 g, 3.56 mmol) in toluene (100 mL). A pale orange solution resulted which was stirred at room temperature overnight. Toluene was evaporated under reduced pressure, and *n*-hexane (50 mL) was then added. A yellow solid was collected on a filter and dried *in vacuo* (2.31 g, 56%). Anal. Calcd for **5**, C<sub>60</sub>H<sub>82</sub>Mn<sub>3</sub>O<sub>12</sub>: C, 62.23; H, 7.09. Found: C, 62.62; H, 7.17. IR (selected values, cm<sup>-1</sup>): 1592 (s; s); 1250 (s; s); 1210 (s; s); 1162 (s; s); 1126 (s; s); 1070 (s; b); 974 (s; b); 830 (s; s); 779 (m; s); 532 (m; s). MW (cryoscopy in benzene): calcd 1159, found 1112.

**Synthesis of 6.** [Fe<sub>2</sub>Mes<sub>4</sub>] (1.87 g, 3.16 mmol) was added portionwise to a cold (–30 °C) solution of **2** (1.79 g, 3.11 mmol) in *n*-hexane (70 mL). A deep red solution resulted which was warmed back to room temperature and stirred overnight. A brownish solution with a yellow-brown microcrystalline solid resulted which was stored at –25 °C for 3 h. The yellow-brown solid was then collected on a filter and dried *in vacuo*. Mass 2.35 g (65%). Anal. Calcd for **6**, C<sub>60</sub>H<sub>82</sub>Fe<sub>3</sub>O<sub>12</sub>: C, 61.95; H, 7.05. Found: C, 61.79; H, 7.24. IR

- (6) (a) Chisholm, M. H.; Rothwell, I. P. In *Comprehensive Coordination Chemistry*; Wilkinson, G., Gillard, R. D., McCleverty J. A., Eds.; Pergamon: Oxford, 1987. (b) Chisholm, M. H. *Chemtracts Inorg. Chem.* **1992**, *4*, 273. (c) Reetz, M. In *Organometallics in Synthesis*; Schlosser, M., Ed.; Wiley: Chichester, 1994; pp 195–282. (d) *Early Transition Metal Clusters with  $\pi$ -Donor Ligands*; Chisholm, M. H., Ed.; VCH: New York, 1995. (e) Parkin, B. C.; Clark, J. R.; Visciglio, V. M.; Fanwick, P. E.; Rothwell, I. P. *Organometallics* **1995**, *14*, 3002. (f) Clark, J. R.; Fanwick, P. E.; Rothwell, I. P. *J. Chem. Soc., Chem. Commun.* **1995**, 553. (g) Yu, J. S.; Ankianiec, B. C.; Rothwell, I. P.; Nguyen, M. T. *J. Am. Chem. Soc.* **1992**, *114*, 1927. (h) Chesnut, R. W.; Jacob, G. G.; Yu, J. S.; Fanwick, P. E.; Rothwell, I. P. *Organometallics* **1991**, *10*, 321. (i) Bonanno, J. B.; Lobkovsky, E. B.; Wolczanski, P. T. *J. Am. Chem. Soc.* **1994**, *116*, 11159. (j) Miller, R. L.; Toreki, R.; LaPointe, R. E.; Wolczanski, P. T.; Van Duyne, G. D.; Roe, D. C. *J. Am. Chem. Soc.* **1993**, *115*, 5570. (k) Durfee, L. D.; Rothwell, I. P. *Chem. Rev.* **1988**, *88*, 1059. The review contains references also to the related Zr-alkoxy-based organometallic chemistry.
- (7) (a) Treichel, P. M. In *Comprehensive Organometallic Chemistry II*; Abel, E. W., Stone, F. G. A., Wilkinson, G., Eds.; Pergamon: Oxford, 1995; Vol. 6, Chapter 3. (b) Whitmire, K. H. In *Comprehensive Organometallic Chemistry II*; Abel, E. W., Stone, F. G. A., Wilkinson, G., Eds.; Pergamon: Oxford, 1995; Vol. 7, Chapter 1.
- (8) Press, W. H.; Flannery, B. P.; Teukolsky, S. A.; Vetterling, W. T. *Numerical Recipes*; Cambridge University Press: Cambridge, UK, 1989.

- (9) Solari, E.; Musso, F.; Gallo, E.; Floriani, C.; Re, N.; Chiesi-Villa, A.; Rizzoli, C. *Organometallics* **1995**, *14*, 2265.
- (10) Klose, A.; Solari, E.; Floriani, C.; Chiesi-Villa, A.; Rizzoli, C.; Re, N. *J. Am. Chem. Soc.* **1994**, *116*, 9123.

**Table 1.** Experimental Data for the X-ray Diffraction Studies on Crystalline Complexes **5** and **6**

	<b>5</b>	<b>6</b>
empirical formula	C <sub>60</sub> H <sub>82</sub> Mn <sub>3</sub> O <sub>12</sub>	C <sub>60</sub> H <sub>82</sub> Fe <sub>3</sub> O <sub>12</sub>
<i>a</i> , Å	10.289(5)	9.748(12)
<i>b</i> , Å	20.878(5)	26.05(3)
<i>c</i> , Å	14.015(5)	12.50(2)
$\beta$ , deg	93.18(2)	107.50(2)
<i>V</i> , Å <sup>3</sup>	3003(3)	3027(8)
<i>Z</i>	2	2
fw	1160.1	1162.8
space group	<i>P</i> 2 <sub>1</sub>	<i>P</i> 2 <sub>1</sub>
<i>T</i> , °C	-123	-123
$\lambda$	0.710 73	0.710 73
$\rho_{\text{calc}}$ , g cm <sup>-3</sup>	1.283	1.276
$\mu$ , mm <sup>-1</sup>	0.679	0.767
no. of reflcns colld	5810	4327
no. of obsd reflcns	3403	2497
( <i>F</i> > 4 $\sigma$ ( <i>F</i> ))		
final <i>R</i> <sup>a</sup> , w <i>R</i> <sup>b</sup>	0.057, 0.056	0.063, 0.072
GOF <sup>c</sup>	1.06	1.11

<sup>a</sup>  $R = \sum |F_o - F_c| / \sum (F_o)$ . <sup>b</sup>  $wR = [\sum (w|F_o - F_c|)^2 / \sum (wF_o^2)]^{1/2}$ . <sup>c</sup>  $GOF = [\sum (w|F_o - F_c|^2) / (N_o - N_v)]^{1/2}$ .

(selected values, cm<sup>-1</sup>): 1592 (s; s); 1253 (s; s); 1230 (s; s); 1210 (s; s); 1162 (s; s); 1119 (s; s); 1070 (s; b); 978 (s; b); 828 (s; s); 778 (m; s); 532 (m; s).

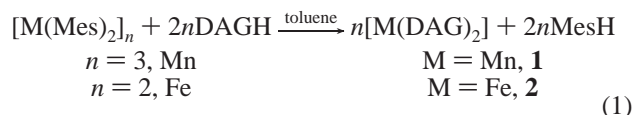
**X-ray Crystallography for Complexes 3, 5, and 6.** The crystals of compounds **3**, **5**, and **6** are all air-sensitive, and they were mounted in glass capillaries and sealed under nitrogen. All data were collected on a Siemens P4 diffractometer, with graphite-monochromatized Mo K $\alpha$  radiation ( $\lambda = 0.710 73$  Å), at room temperature for **3** and at 150 K for **5** and **6**. The intensities were measured using the  $\omega$  scan type, with a scan range of 1.6° for **5** and of 1.4° for **6**, with variable scan speed;  $2\theta$  range 2–50° ( $0 \leq h \leq 10$ ,  $0 \leq k \leq 25$ ,  $-16 \leq l \leq 16$ ), and 3–45° ( $0 \leq h \leq 10$ ,  $0 \leq k \leq 28$ ,  $-13 \leq l \leq 12$ ), for complexes **5** ( $R_{\text{int}}$  3.8%) and **6** ( $R_{\text{int}}$  7.9%), respectively. No absorption correction was applied. The structures were solved using the SIR92 program<sup>11</sup> and refined with the SHELXTL IRIS package.<sup>12</sup> The full-matrix least-squares refinement method was applied, and the quantity minimized was  $\sum w(F_o - F_c)^2$ . Coordinates and anisotropic thermal parameters were refined for the non-hydrogen atoms, while the hydrogen atoms were located in calculated positions and refined riding on the corresponding atoms with isotropic *U*. The weighting scheme was  $w^{-1} = \sigma^2(F) + aF^2$  ( $a = 0.0009$  for **5** and 0.0022 for **6**). The relevant information about the data collection and refinement of the structures of complexes **5** and **6** is summarized in Table 1. The solution of complex **3** was carried out in the space group *P*4<sub>1</sub> [unit cell parameters:  $a = 15.556(3)$  Å,  $c = 37.901(8)$  Å,  $Z = 4$ ], and the molecular structure was clearly indicated, but the refinement did not converge to acceptable agreement factors. All attempts at solving or refining the structure in other possible space groups failed to yield better results.

## Results and Discussion

Despite the enormous amount of early transition metal–alkoxo complexes,<sup>6</sup> only a few examples regarding the complexation of manganese(II) and iron(II) by alkoxo ligands are known.<sup>13</sup> Their synthesis is normally achieved by protonolysis

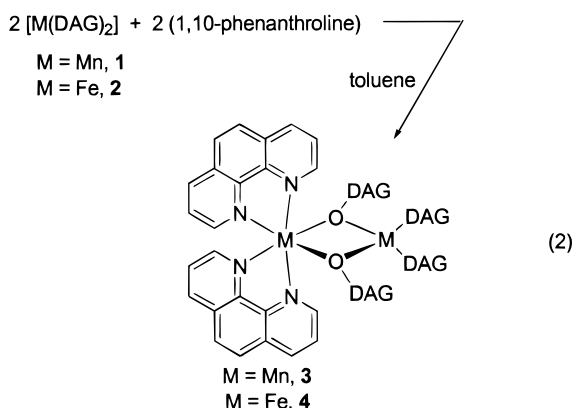
of the amido or alkyl derivatives. Homoleptic alkoxo- and phenoxo-Mn complexes are usually amorphous air-sensitive polymers<sup>14</sup> unless they have very bulky substituents. In this latter case, crystalline solids have been obtained, and the structure has been determined for [Mn<sub>3</sub>(OCH–Bu<sup>t</sup>)<sub>6</sub>]<sup>15</sup> and [Mn{O(2,4,6-Bu<sup>t</sup>C<sub>6</sub>H<sub>2</sub>)<sub>2</sub>}]<sub>2</sub>.<sup>16</sup> In the case of iron(II), alkoxo complexes are even more rare.<sup>7a,13d</sup> The first to be structurally determined was that of the Mn analogue [Fe{O(2,4,6-Bu<sup>t</sup>-C<sub>6</sub>H<sub>2</sub>)<sub>2</sub>}]<sub>2</sub>, the two complexes being isostructural.<sup>16</sup> The poor chemistry of Mn<sup>II</sup>– and Fe<sup>II</sup>–alkoxo complexes is probably due both to difficulty in obtaining pure crystalline materials and to their exceedingly high oxygen sensitivity.

The synthesis of Mn<sup>II</sup>– and Fe<sup>II</sup>–DAG derivatives was performed using the organometallic methodology employing the protonolysis of Mn<sub>3</sub>Mes<sub>6</sub><sup>9</sup> and Fe<sub>2</sub>Mes<sub>4</sub><sup>10</sup> by DAGH in toluene (see eq 1).



Reaction 1 afforded the very soluble air-sensitive DAG complexes **1** and **2**, which were purified by recrystallization from *n*-hexane at low temperature. The MW determinations in benzene (cryoscopy) support a monomeric form for **1** and **2** in solution. Since the molecular complexity of **1** and **2** in the solid state could not be determined with an X-ray analysis, useful information was derived from the analysis of their magnetic properties (see below). We can anticipate, however, that though the Mn(II) and Fe(II) derivatives have the same behavior in solution, their solid state complexity seems to be very much different. Simple derivatization of **1** and **2** was pursued with the purpose of getting more information on how the [Mn–(DAG)<sub>2</sub>] unit can aggregate in solution and in the solid state, and how to derive structural information.

Reaction of **1** and **2** with 1,10-phenanthroline in toluene afforded [M<sub>2</sub>(DAG)<sub>4</sub>(Phen)<sub>2</sub>] [M = Mn (**3**), Fe (**4**)] (eq 2) which proved to have the same structure based on spectral similarities (IR and magnetic properties, see below).



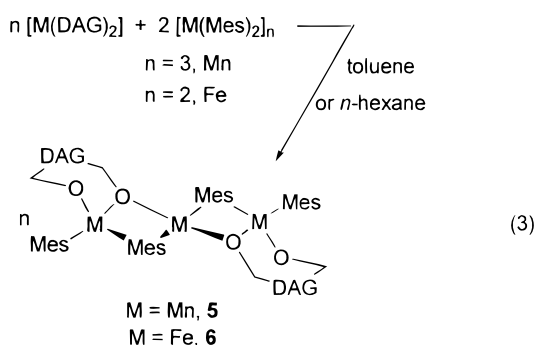
Complex **3** was obtained as orange-amber crystals which are readily soluble in methylene chloride and THF and partially soluble in toluene (from which crystals suitable for X-ray

- (11) Altomare, A.; Cascarano, G.; Giacovazzo, C.; Guagliardi, A.; Burla, M. C.; Polidori, G.; Camalli, M. *J. Appl. Crystallogr.* **1994**, *27*, 435.  
 (12) Sheldrick, G. M. *SHELXTL Iris*; Siemens Analytical X-ray Instruments Inc.: Madison, WI, 1990.  
 (13) (a) Bradley, D. C.; Mehrotra, R. C.; Gaur, D. P. *Metal Alkoxides*; Academic: New York, 1978. (b) Mehrotra, R. C. *Adv. Inorg. Chem. Radiochem.* **1983**, *26*, 269. (c) Chiswell, B.; McKenzie, E. D.; Lindoy, L. F. In *Comprehensive Coordination Chemistry*; Wilkinson, G., Gillard, R. D., McCleverty, J. A., Eds.; Pergamon: Oxford, 1987; Vol. 4, Chapter 41. (d) Hawker, P. N.; Twigg, M. V. In *Comprehensive Coordination Chemistry*; Wilkinson, G., Gillard, R. D., McCleverty, J. A., Eds.; Pergamon: Oxford, 1987; Vol. 4, Chapter 44.1.

- (14) Horvath, B.; Mösele, R.; Horvath, E. G. *Z. Anorg. Allg. Chem.* **1979**, *449*, 41.  
 (15) Murray, B. D.; Hope, H.; Power, P. P. *J. Am. Chem. Soc.* **1985**, *107*, 169.  
 (16) Bartlett, R. A.; Ellison, J. J.; Power, P. P.; Shoner, S. C. *Inorg. Chem.* **1991**, *30*, 2888 and references therein.

diffraction were obtained) or diethyl ether. Iron complex **4** was obtained as a blue-purple powder soluble in methylene chloride and THF, but insoluble in diethyl ether or toluene. Though the data are rather poor, the X-ray analysis of **3** established the existence of the atom connectivity, showing the nonsymmetric binding of the DAG and phenanthroline ligands, as reported in eq 2. Two structural parameters may eventually be of interest: the Mn···Mn distance [3.14 Å] and the Mn–O–Mn angles (ca. 97°).

The special role played by the iron–carbon functionality in a chiral environment<sup>17</sup> prompted us to take advantage of the presence of chiral ancillary ligands around manganese(II) and iron(II) in complexes **1** and **2**. Their organometallic derivatization was not so easy to achieve. The reaction of **1** and **2** with lithium alkyls and Grignard reagents, with the purpose to produce “ate” complexes, led to the scrambling of the ligands, thus forming intractable mixtures. The results mentioned above are the consequence of the kinetic lability of Mn(II) and Fe(II) in such environments. As a matter of fact, the presence of kinetic lability prompted us to use the synthetic procedure summarized in eq 3. After recrystallization in *n*-hexane, the



reaction in toluene (for manganese) or *n*-hexane (for iron) afforded the microcrystalline trimeric mixed alkoxy-aryl complexes **5** (yellow-amber) and **6** (greenish-yellow), both extremely air sensitive solids. The trimeric structure present in the solid state (see below) is also retained in solution, as witnessed by molecular weight determination (cryoscopy in benzene). A more straightforward synthesis of **5** and **6** can be performed reacting  $\text{Mn}_3\text{Mes}_6$  and  $\text{Fe}_2\text{Mes}_4$  with the appropriate amount of [DAGH]. This synthetic approach was successfully used in the reaction of  $[\text{Mn}(\text{PhCMe}_2\text{CH}_2)_2]_2$  with 2,4,6- $\text{Bu}_3\text{C}_6\text{H}_2\text{OH}$ ,<sup>18</sup> and  $[\text{M}\{\text{CH}(\text{SiMe}_3)_2\}_2]_2$  with 2,6- $\text{Bu}^i_2\text{-4-MeC}_6\text{H}_2\text{OH}$ .<sup>19</sup>

The structures of complexes **5** and **6** turned out to be very similar. Only the complete molecular structure of **5** is shown in Figure 1, and some selected bond distances and angles are listed in Table 2 for both compounds. The molecules consist of an almost linear sequence of three metal atoms [ $\text{Mn1-Mn2-Mn3} = 170.8(1)^\circ$  and  $\text{Fe1-Fe2-Fe3} = 169.8(2)^\circ$ ], each in a distorted tetrahedral coordination, with two terminal and two bridging mesityl groups, and two DAG ligands. As in other analogous DAG complexes,<sup>1,2</sup> both DAG units form six-membered O1, O6 chelating rings with M1 and M3, respectively, while O1a and O1b bridge M1, M2 and M2, M3, respectively.

The metal to metal nonbonding distances are  $\text{Mn1}\cdots\text{Mn2} = 2.930(3)$  Å,  $\text{Mn2}\cdots\text{Mn3} = 2.927(4)$  Å,  $\text{Fe1}\cdots\text{Fe2} = 2.878(6)$

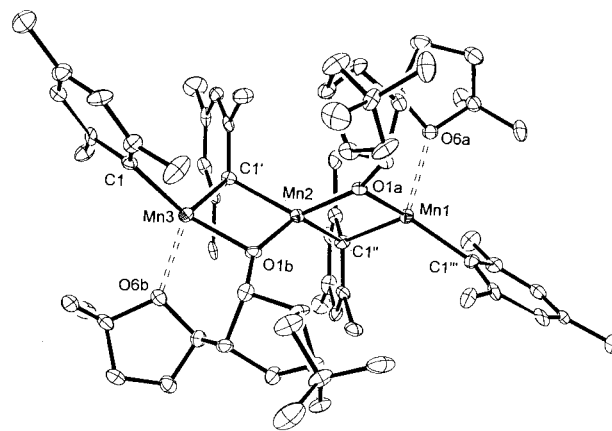


Figure 1. ORTEP drawing of complex **5** (50% probability ellipsoids).

Table 2. Selected Bond Lengths (Å) and Angles (deg) for Complexes **5** and **6**

5		6	
Mn(1)···Mn(2)	2.930(3)	Fe(1)···Fe(2)	2.878(6)
Mn(1)–O(1a)	2.067(7)	Fe(1)–O(1a)	2.000(12)
Mn(1)–O(6a)	2.300(8)	Fe(1)–O(6a)	2.328(13)
Mn(1)–C(1')	2.272(11)	Fe(1)–C(1'')	2.210(19)
Mn(1)–C(1''')	2.101(11)	Fe(1)–C(1''')	2.047(21)
Mn(2)···Mn(3)	2.927(4)	Fe(2)···Fe(3)	2.881(7)
Mn(2)–O(1a)	2.034(7)	Fe(2)–O(1a)	2.005(12)
Mn(2)–O(1b)	2.024(7)	Fe(2)–O(1b)	1.997(12)
Mn(2)–C(1')	2.264(11)	Fe(2)–C(1')	2.168(22)
Mn(2)–C(1'')	2.253(11)	Fe(2)–C(1'')	2.236(17)
Mn(3)–O(1b)	2.055(7)	Fe(3)–O(1b)	1.999(14)
Mn(3)–O(6b)	2.238(8)	Fe(3)–O(6b)	2.295(12)
Mn(3)–C(1)	2.110(11)	Fe(3)–C(1)	2.062(20)
Mn(3)–C(1')	2.277(11)	Fe(3)–C(1')	2.177(18)
O(1a)–Mn(1)–O(6a)	79.9(3)	O(1a)–Fe(1)–O(6a)	79.9(5)
O(1a)–Mn(1)–C(1'')	93.2(4)	O(1a)–Fe(1)–C(1'')	93.9(6)
O(6a)–Mn(1)–C(1''')	109.3(4)	O(6a)–Fe(1)–C(1''')	97.7(6)
C(1'')–Mn(1)–C(1''')	115.0(4)	C(1'')–Fe(1)–C(1''')	116.7(7)
Mn(1)···Mn(2)···Mn(3)	170.8(1)	Fe(1)···Fe(2)···Fe(3)	169.8(2)
O(1a)–Mn(2)–O(1b)	101.9(3)	O(1a)–Fe(2)–O(1b)	100.6(5)
O(1b)–Mn(2)–C(1')	94.5(4)	O(1b)–Fe(2)–C(1')	92.3(6)
O(1a)–Mn(2)–C(1'')	94.7(4)	O(1a)–Fe(2)–C(1'')	93.0(6)
C(1')–Mn(2)–C(1'')	104.4(4)	C(1')–Fe(2)–C(1'')	103.9(7)
O(1b)–Mn(3)–O(6b)	81.1(3)	O(1b)–Fe(3)–O(6b)	80.4(5)
O(6b)–Mn(3)–C(1)	115.0(4)	O(6b)–Fe(3)–C(1)	100.3(6)
O(1b)–Mn(3)–C(1')	93.2(4)	O(1b)–Fe(3)–C(1')	92.0(7)
C(1)–Mn(3)–C(1')	113.6(4)	C(1)–Fe(3)–C(1')	115.5(8)
Mn(1)–O(1a)–Mn(2)	91.2(3)	Fe(1)–O(1a)–Fe(2)	91.9(4)
Mn(2)–O(1b)–Mn(3)	91.7(3)	Fe(2)–O(1b)–Fe(3)	92.3(6)
Mn(2)–C(1')–Mn(3)	80.3(3)	Fe(2)–C(1')–Fe(3)	83.1(7)
Mn(1)–C(1'')–Mn(2)	80.7(3)	Fe(1)–C(1'')–Fe(2)	80.7(6)

Å,  $\text{Fe2}\cdots\text{Fe3} = 2.881(7)$  Å. The dihedral angle between the two four-membered rings formed by the metals and the bridging atoms is  $64^\circ$  for the Mn(II) complex and  $59^\circ$  for the Fe(II) complex, quite far from the ideal  $90^\circ$  of a regular tetrahedron. Such a distortion may be ascribed to the steric effects of the two DAG's which are located on the same side when viewing along the M–M–M line. Figure 2 shows this situation for the Fe(II) complex and indicates the presence of a cavity between the two sugars, which is preserved in the crystal packing. Four oxygen atoms, O1a, O1b, O3a, and O3b, with a flattened tetrahedral geometry, face the cavity with a nonbonding distance  $\text{O3a}\cdots\text{O3b}$  of 4.7 Å for **5** and of 3.6 Å for **6**; the cavity for the Mn(II) derivative is therefore considerably larger than that of the Fe(II) compound. The bridging mesityl groups are almost perpendicular to the M–C1–M–O1 planes and form a (2e,3c) system with an average M–C1–M angle of  $81^\circ$ . The terminal and bridging Mn–C and Fe–C distances are quite close to those found in the parent  $[\text{Mn}_3\text{Mes}_6]_9$  and  $[\text{Fe}_2\text{Mes}_4]_{10}$  compounds.

(17) Pearson, A. J. *Iron Compounds in Organic Synthesis*; Academic: San Diego, 1994.

(18) Jones, R. A.; Koschmieder, S. U.; Nunn, C. M. *Inorg. Chem.* **1988**, *27*, 4526.

(19) Hitchcock, P. B.; Lappert, M. F.; Leung, W.-P.; Buttrus, N. H. J. *Organomet. Chem.* **1990**, *394*, 57.

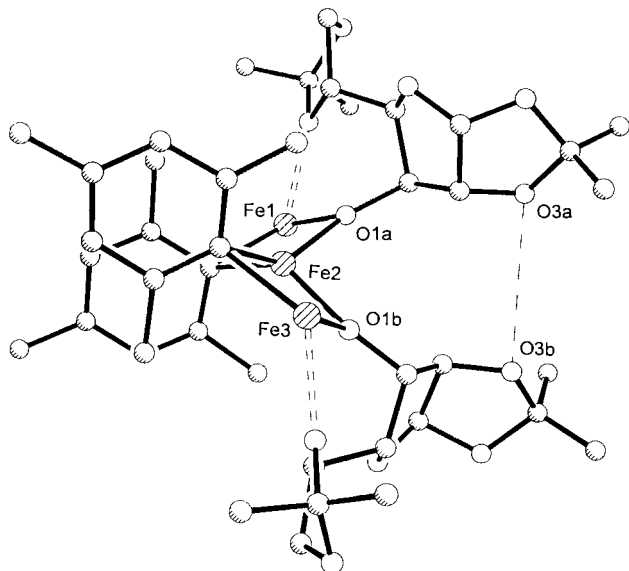


**Figure 2.** View of complex **6** showing the cavity formed by the two DAG moieties.

Significant structural features of the Mn<sup>II</sup>- and Fe<sup>II</sup>-DAG complexes were inferred from the accurate analysis of the magnetic data. Magnetic susceptibility data for complexes **1**–**6** were collected in the temperature range 1.9–300 K. The magnetic moment of **1** (Figure 3a) at room temperature, 5.65 BM at 298 K, is slightly lower than the value expected for a magnetically dilute  $S = 5/2$  ion. On lowering the temperature, the magnetic moment decreases first gradually and then sharply reaching a value of 2.55 BM at 1.9 K. This behavior is clearly not compatible with a monomeric structure for which a constant magnetic moment down to low temperatures is expected due to the very small zero-field splitting of Mn(II). Moreover, no acceptable fitting could be obtained using the equation for two coupled  $S = 5/2$  ions.<sup>20</sup> Therefore, the magnetic behavior of **1** excludes the possibility of a monomeric or a dimeric structure, rather suggesting a cluster with a higher nuclearity.

For complex **2** (Figure 3b) the magnetic moment per iron remains essentially constant (ca. 5.3 BM) from 300 to about 60 K and then suddenly decreases reaching a value of 3.41 BM at 1.9 K. As Fe(II) ions may have a relevant zero-field splitting,<sup>21,22</sup> the magnetic behavior of **2** is compatible with a monomeric structure, although only a poor fitting could be obtained using a simple  $S = 2$  spin Hamiltonian with an axial zero-field-splitting.

The data for the dimer complex **3** (Figure 4a) were fitted with the simple theoretical equation<sup>20</sup> obtained assuming that the interaction between the two spin centers were described by the Heisenberg spin Hamiltonian  $H_{\text{ex}} = -2J\hat{S}_1 \cdot \hat{S}_2$ , with  $S_1 = S_2 = 5/2$ . To obtain a good fitting we included a correction for the presence of monomeric Mn(II) impurities which were assumed to obey Curie law. The following equation is therefore obtained for the total susceptibility:

$$\chi = \frac{1}{2}(1 - \chi)\chi_{\text{dim}} + \kappa \frac{Ng^2\mu_B^2 S(S+1)}{3kT}$$

where  $S = 5/2$ ,  $g$  is the  $g$  factor of the impurity (assumed to be

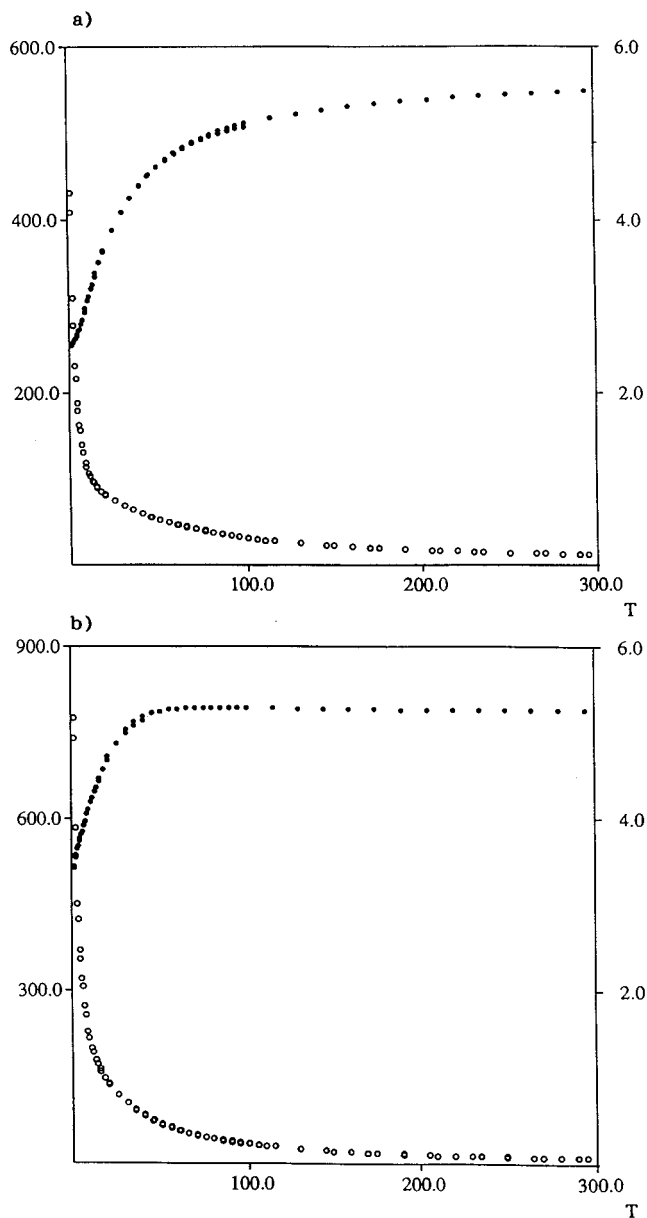


**Figure 3.** Magnetic susceptibilities (○) and magnetic moments (●), as a function of temperature for complexes **1** (a) and **2** (b).

2.00), and  $\kappa$  is the monomeric impurity fraction. A good fit to the collected data,  $R = 9 \times 10^{-4}$ , was obtained for  $g = 1.98$ ,  $J = -3.2 \text{ cm}^{-1}$ , and  $x = 0.8\%$  (see solid and dashed lines in Figure 4a).

For the iron dimer **4** (Figure 4b) the magnetic moment per Fe steadily increases from room temperature down to about 20 K and then suddenly decreases. The increase is due to a ferromagnetic coupling of the two iron centers, while the decrease at low temperatures is due to zero-field splitting, which is known to be relevant for Fe(II) species. These data were fitted using the following spin Hamiltonian:

$$\hat{H} = g\mu_B\mathbf{H} \cdot \hat{S}_1 + g\mu_B\mathbf{H} \cdot \hat{S}_2 + D[\hat{S}_{1z}^2 - 2(2+1)/3] + D[\hat{S}_{2z}^2 - 2(2+1)/3] - 2J(\hat{S}_1 \cdot \hat{S}_2)$$

where  $S_1$  and  $S_2$  are the spin of the two iron ions, both being 2,  $D$  is the zero-field-splitting parameter, and  $J$  is the Heisenberg coupling constant between the two Fe(II) ions. Although the structure of **4** shows nonequivalent Fe(II) centers,

(20) O'Connor, C. J. *Progr. Inorg. Chem.* **1982**, 29, 203.

(21) Carlin, R. L. *Magnetochemistry*; Springer: Berlin, Germany, 1986.

(22) Casey, A. T.; Mitra, S. In *Theory and Applications of Molecular Paramagnetism*; Bodreaux, E. A., Mulay, L. N., Eds.; Wiley: New York, 1976; p 135.

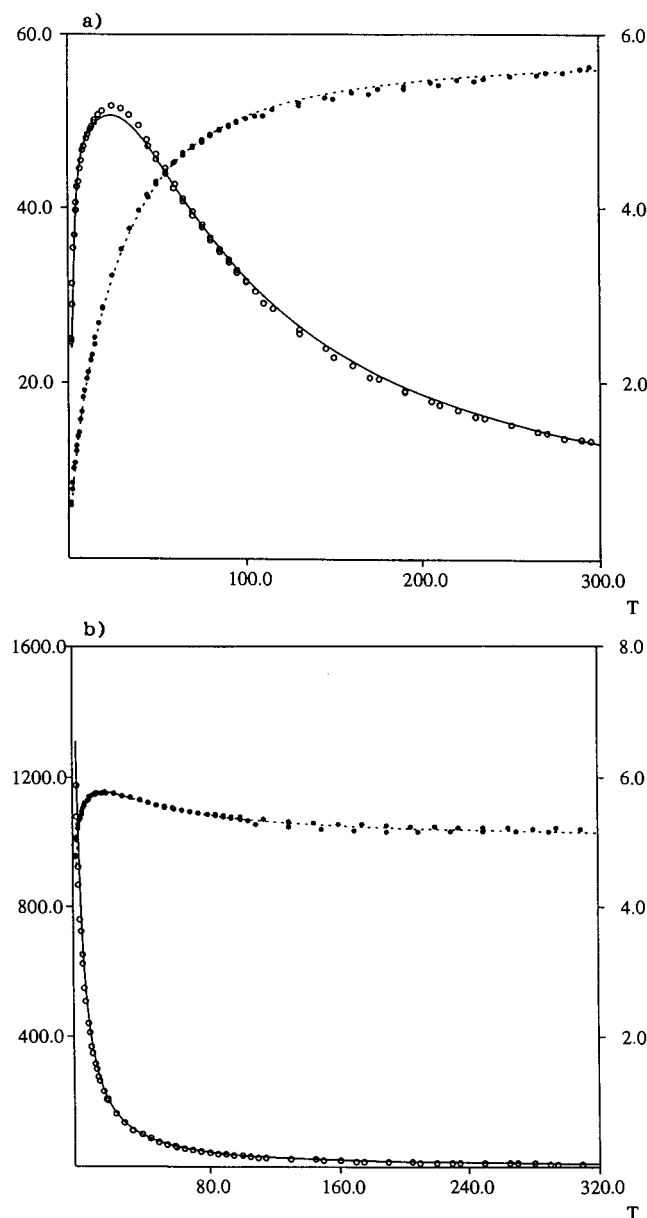


**Figure 4.** Magnetic susceptibilities (○) and magnetic moments (●), as a function of temperature for complexes **3** (a) and **4** (b).

we assumed equivalent  $g$  factors and  $D$  values for the two irons, to avoid overparametrization. The susceptibility for such a system is calculated using the thermodynamic relationship  $\chi = M/H$ , where the magnetization  $M$  is given by<sup>23</sup>

$$M = \frac{N \sum_i (-dE_i/dH) \exp(-E_i/kT)}{\sum_i \exp(-E_i/kT)}$$

The energy levels of the dimer,  $E_i$ , are evaluated by diagonalizing the Hamiltonian matrix ( $25 \times 25$ ) in the basis constituted by the products of the spin functions for the two  $S = 2$  centers. The best fit parameters,  $R = 5 \times 10^{-4}$ , are  $g = 2.10$ ,  $J = +2.1 \text{ cm}^{-1}$ ,  $D = +7.3 \text{ cm}^{-1}$  (see solid and dashed lines in Figure 4b).

The coupling constant value found for complex **3** ( $-3.2 \text{ cm}^{-1}$ ) shows a small antiferromagnetic coupling for this di- $\mu$ -alkoxo

Mn(II) species. This value is consistent with those usually found for  $\mu$ -alkoxo and  $\mu$ -carboxylato Mn(II)–Mn(II) dimers<sup>24</sup> intensively studied within the investigation of inorganic model complexes of manganese-containing metalloproteins.<sup>25</sup> The fitting for the iron dimer **4** shows a small ferromagnetic coupling ( $2.1 \text{ cm}^{-1}$ ). This value is in the range of those observed for most of the oxygen bis-bridged diferrous complexes, which have Fe–O–Fe angles close to  $90^\circ$  and show a ferromagnetic coupling lower than  $10 \text{ cm}^{-1}$ .<sup>26</sup> Moreover, such a result supports the hypothesis of structural analogy between compound **4** and the X-ray characterized **3**. Indeed, the oxygen bis-bridged manganese dimer **3** presents Mn–O–Mn angles close to  $90^\circ$ , and the same structure, with bis-bridged Fe(II) ions, would have a magnetic behavior perfectly compatible with that actually observed for **4**.

When we consider the trimeric complex **5** (Figure 5a), the temperature dependence of  $\mu_{\text{eff}}$  shows a plateau at about  $3.7 \mu_{\text{B}}$  below 100 K and a limited increase above 150 K reaching a room temperature value,  $4.71 \mu_{\text{B}}$  at 295 K, which is much smaller than expected for three uncoupled Mn(II) ions. This behavior clearly indicates a strong antiferromagnetic coupling between the three Mn(II) centers, with spin frustration, leading to an overall  $S = 5/2$  ground state. These data were fitted using the theoretical equation corresponding to the following spin Hamiltonian:

$$\hat{H} = -2J(\hat{S}_c \cdot \hat{S}_{t1} + \hat{S}_c \cdot \hat{S}_{t2}) + g\mu_{\text{B}}\mathbf{H} \cdot \hat{S}$$

where  $S_c$  is the spin of the central ion,  $S_{t1}$  and  $S_{t2}$  are the spin of the terminal ions, all being  $5/2$ , and  $S$  is the total spin. In this Hamiltonian we assumed equivalent  $g$  factors for the three ions and neglected the coupling between the two terminal ions, both approximations being quite reasonable on the basis of the structure. The spin energy levels may be calculated by Kambe methods,<sup>27</sup> which gives

$$E(S', S) = -J[S(S+1) - S'(S'+1) - s(s+1)]$$

in which  $s = 5/2$  and  $S'$  is the quantum number corresponding to  $\hat{S}' = \hat{S}_{t1} + \hat{S}_{t2}$ . We use the expression obtained by inserting these energy levels in the Van Vleck equation<sup>28</sup> to fit the temperature dependence of  $\mu_{\text{eff}}$ . A good fit,  $R = 3 \times 10^{-4}$ , was obtained for  $g = 2.09$  and  $J = -17.6 \text{ cm}^{-1}$  and is shown in Figure 5a. In terms of the energy level scheme, the results above indicate that the  $S = 5/2$  ground state is well isolated with the next excited levels ( $S = 3/2$  at  $44.0 \text{ cm}^{-1}$  and  $S = 7/2$  at  $61.6 \text{ cm}^{-1}$ ) so high in energy as to be negligibly populated at low temperatures.

The trimeric complex **6** (Figure 5b) shows a temperature dependence of the magnetic moment above 50 K analogous to that of **5**, with a plateau at about  $3.7 \mu_{\text{B}}$  below 100 K and a slow increase to a room temperature value,  $4.39 \mu_{\text{B}}$  at 295 K, much smaller than expected for three uncoupled Fe(II) ions. However, in this case, there is a sudden decrease of the magnetic moment below 50 K, with a value of  $2.95 \mu_{\text{B}}$  at 1.9 K. The

(24) (a) Menage, S.; Vitols, S. E.; Bergerat, P.; Codjovi, E.; Kahn, O.; Girerd, J.-J.; Guillot, M.; Solans, X.; Calvet, T. *Inorg. Chem.* **1991**, *30*, 2666. (b) Wiegart, K.; Bossek, K.; Nuber, B.; Weiss, J.; Bonvoisin, J.; Corbella, M.; Vitols, S. E.; Girerd, J.-J. *J. Am. Chem. Soc.* **1988**, *110*, 7398. (c) Wiegart, K.; Bossek, K.; Bonvoisin, J.; Beauvillain, P. *Angew. Chem., Int. Ed. Engl.* **1986**, *25*, 1030.

(25) Wiegart, K. *Angew. Chem., Int. Ed. Engl.* **1989**, *28*, 1153.

(26) Hendrich, M. P.; Edmund, P. D.; Wang, C.-P.; Synder, B. S.; Holm, R. H.; Münck, E. *Inorg. Chem.* **1994**, *33*, 2848 and references therein.

(27) Kambe, K. *J. Phys. Jpn.* **1950**, *5*, 48.

(28) Van Vleck, J. H. *The Theory of Electric and Magnetic Susceptibilities*; Oxford University Press: Oxford, UK, 1932.

(23) Kahn, O. *Molecular Magnetism*; VCH: New York, 1993.

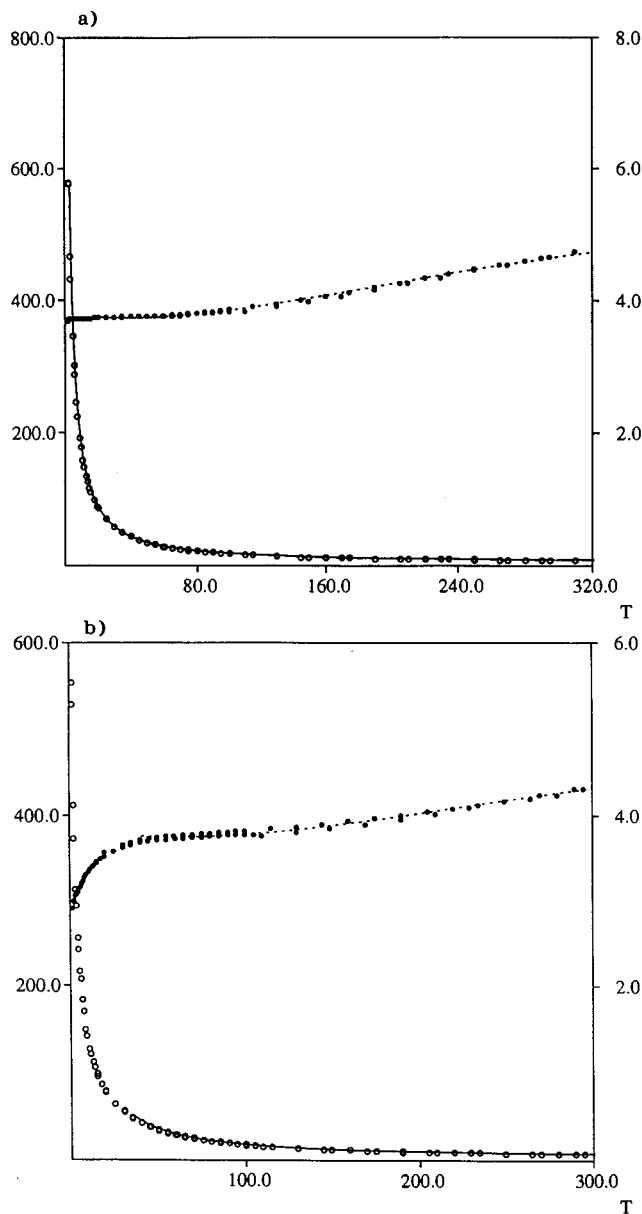


**Figure 5.** Magnetic susceptibilities (○) and magnetic moments (●), as a function of temperature for complexes **5** (a) and **6** (b).

behavior above 50 K still indicates a strong antiferromagnetic coupling between the three Fe(II) centers, with spin frustration, leading to an overall  $S = 2$  ground state. This behavior is completely analogous to that observed for the manganese trimer **5**, as expected on the basis of essentially the same X-ray structure. The decrease at low temperatures is due to the zero-

field-splitting of the iron(II) centers, which is known to be much higher than for Mn(II).<sup>21,22</sup> The data from 300 to 50 K were fitted using the spin Hamiltonian of eq 2 and following the same procedure used for **5**. The best fit was obtained for  $g = 2.59$  and  $J = -37.6 \text{ cm}^{-1}$  and is shown in Figure 5b. The low temperature data from 1.8 to 50 K were reasonably well fitted to a spin Hamiltonian for a single spin center with  $S = 2$ , including axial zero-field splitting, and led to  $g = 2.60$  and  $D = 6.5 \text{ cm}^{-1}$ . The calculated values of  $g$  and  $D$  are quite high but still in the range of values observed for the highly anisotropic Fe(II) ion.<sup>21,22</sup>

The  $J$  values found for the trimeric compounds **5** and **6** ( $-17.6$  and  $-37.6 \text{ cm}^{-1}$ , respectively) indicate a fairly strong antiferromagnetic coupling for both  $\mu$ -alkoxo  $\mu$ -mesityl bis-bridged Mn(II) or Fe(II) species. Only very few  $\mu$ -mesityl bis-bridged Mn(II) and Fe(II) compounds have been magnetically characterized and show coupling constant values between  $-30$  and  $-60 \text{ cm}^{-1}$ . The slightly smaller interaction observed for **5** and **6** is probably due to the presence of only one bridging mesityl, the other bridge being a  $\mu$ -alkoxo which is known to lead to small ferromagnetic interactions for Mn(II) species.

### Conclusions

The protolysis of Mn(II) and Fe(II) organometallics with DAGH led to quite rare homoleptic chiral diacetoneglucose derivatives  $[\text{M}(\text{DAG})_2]$  [ $\text{M} = \text{Mn}, \text{Fe}$ ]. Their monomeric nature in solution is maintained in the solid state, for the iron derivative, while the magnetic analysis showed a higher molecular complexity for  $[\text{Mn}(\text{DAG})_2]$ . The organometallic functionalization of a metal center bonded to chiral ancillary ligands is of primary importance in metal-assisted stereoselective synthesis. In the case of Mn-DAG and Fe-DAG derivatives, the formation of Mn-C and Fe-C bonds in the presence of chiral alkoxo ligands was achieved using a ligand redistribution reaction. Mixed complexes of Mn(II) and Fe(II) were obtained in the form of complexes  $[\text{Mes}_2\text{M}_3(\mu\text{-DAG})_2(\mu\text{-Mes})_2]$  [ $\text{M} = \text{Mn}, \text{Fe}$ ]. The almost linear trimetallic skeleton display a strong antiferromagnetic coupling between the M(II) centers, with a spin frustration leading to an overall  $S = 5/2$  [Mn] and  $S = 2$  [Fe] ground state, respectively.

**Acknowledgment.** We thank the Fonds National Suisse de la Recherche Scientifique (Grant No. 20-46'590.96) and Ciba Specialty Chemicals (Basel) for financial support. G.G. and D.V. acknowledge MURST (40% and 60%) and CNR for funding. The Herbette foundation (N.R., University of Lausanne) is also acknowledged.

**Supporting Information Available:** X-ray crystallographic files, in CIF format, for complexes **5** and **6** are available on the Internet only. Access information is given on any current masthead page.

IC980301Y